2008

A Study of Land Surface Processes Using Land Surface Models Over the Little River Experimental Watershed

A. K. Sahoo
George Mason University

P. A. Dirmeyer
IGES

P. R. Houser
IGES

Menas Kafatos
Chapman University, kafatos@chapman.edu

Recommended Citation

Sahoo, A. K., P. A. Dirmeyer, P. R. Houser, and M. Kafatos (2008), A study of land surface processes using land surface models over the Little River Experimental Watershed, Georgia, J. *Geophys. Res.*, 113, D20121. doi:10.1029/2007JD009671

A Study of Land Surface Processes Using Land Surface Models Over the Little River Experimental Watershed

A study of land surface processes using land surface models over the Little River Experimental Watershed, Georgia

Alok K. Sahoo,[1,2] Paul A. Dirmeyer,[3] Paul R. Houser,[1,2] and Menas Kafatos[1]

Received 3 December 2007; revised 31 March 2008; accepted 7 August 2008; published 30 October 2008.

[1] Three different land surface models (Hydrological improvements to the Simplified version of the Simple Biosphere model (HySSiB), Noah model, and Community Land Model (CLM)) were simulated on the NASA Goddard Space Flight Center's Land Information System platform at 1-km resolution over the Little River Experimental Watershed, Georgia, and the simulated results were analyzed to address the local-scale land-atmosphere processes. All the three models simulated the soil moisture in space and time realistically. The Noah model produced higher soil moisture whereas the CLM got lower soil moisture with many dry down phases. CLM and HySSiB models were oversensitive to the atmospheric events. Different vertical discretizations of the model layers affected the soil moisture results in all the three models. The arithmetic model ensemble mean soil moisture performed reasonably well even at individual in-situ measurement sites. We found that different model schemes partitioned the incoming water and energy differently and hence produced different results for the water and energy budget parameters. In CLM, the energy and water budget parameters were very closely connected to the soil moisture (e.g., evaporation, latent, and sensible heat) change. HySSiB produced very high surface runoff and very low subsurface runoff. The Noah model did not produce much surface and subsurface runoff resulting in high surface soil moisture. We did not find much variability in Noah latent heat, sensible heat, and ground heat fluxes. From soil moisture data assimilation point of view, the mean bias removed Noah soil moisture was found to be better than other data sets.

Citation: Sahoo, A. K., P. A. Dirmeyer, P. R. Houser, and M. Kafatos (2008), A study of land surface processes using land surface models over the Little River Experimental Watershed, Georgia, *J. Geophys. Res.*, *113*, D20121, doi:10.1029/2007JD009671.

1. Introduction

[2] Land surface processes play an integral and substantial part in both global water and energy budgets. Soil moisture is a critical element in all land surface processes. It controls the surface and sub-surface runoff; it supplies moisture to the atmosphere; and helps determine the Bowen ratio [*Dirmeyer*, 1995]. It also acts as a water reservoir for the land surface hydrologic cycle and controls the water uptake by the vegetation above the ground [*Vinnikov and Yeserkepova*, 1991]. Quantifying soil moisture is important for atmospheric scientists, hydrologists, agriculture scientists as well as the policy makers who try to mitigate natural disasters such as floods and droughts.

[3] Yet quantifying soil moisture is very difficult. There is no clear definition of soil moisture. Different researchers and professions look at it from different prospective and define it in many different ways [*Dirmeyer*, 2004]. Nor is there a global data set of observed soil moisture available because the field observations are very scanty, satellites can not see below the soil surface or through vegetation to measure it and the current state-of-the-art land surface models are not capable of representing the complex land surface physics to simulate it accurately [*Reichle et al.*, 2004]. Even if a land surface model (LSM) were sufficiently accurate, it requires complete and accurate meteorological data as input - this is also lacking over most of the globe.

[4] Model intercomparison studies are one of the ways to overcome the problems associated with any single model, since results from the model intercomparison studies are not biased by any individual model. As a result, there have been many model intercomparison studies conducted in the last decade to simulate different land surface variables and address specific science problems related to the land surface hydrology. The Project for Intercomparison of Land Surface Parameterization Schemes (PILPS) is one such model intercomparison project which was established in 1992 and has evaluated the parameterization of energy and water fluxes to/from the land-atmosphere interface using many land surface schemes [*Henderson-Sellers et al.*, 1995]. The Global Soil Wetness Project (GSWP) I and II are other such model intercomparison projects to assess the quality and performance of different land surface schemes (LSS) and estimate land surface variables on global scales

[1]College of Sciences, George Mason University, Fairfax, Virginia, USA.
[2]Center for Research on Environment and Water, IGES, Calverton, Maryland, USA.
[3]Center for Ocean-Land-Atmosphere Studies, IGES, Calverton, Maryland, USA.

0148-0227/08/2007JD009671

[*Dirmeyer et al.*, 1999, 2006]. Another such land surface scheme intercomparison project focused on river hydrology and snow simulation was carried out by *Boone et al.* [2004] over the Rhone River.

[5] Does the complexity of the LSM parameterizations contribute to model performance differences for land surface simulations? Does the model ensemble mean soil moisture from different LSMs perform reasonably better compared to any individual model as concluded by *Guo et al.* [2007]? To answer the above questions, this paper focuses on three different LSMs with different model parameterizations and analyzes the soil moisture simulation results from them over the Little River Experimental Watershed (LREW), Georgia. This paper is the second in the series; in the first work [*Sahoo et al.*, 2008] we compared the Advanced Microwave Scanning Radiometer-Earth Observing System (AMSR-E) satellite retrieved soil moisture results over LREW using two different retrieval methods with the field observed soil moisture data. The first paper was focused on assessment of the observed remote sensing data. In contrast, the present paper focuses on land surface modeling and tries to look further at the roles of model complexity, forcing data sets and land surface conditions in order to answer the differences in the land surface simulation results. Here, we integrate the LSMs generating hourly output at 1-km spatial resolution. The availability of high quality and fine spatial and temporal (every 30 minutes) field observed data sets in this study is advantageous to perform this comprehensive comparison study. Our ultimate objective is to perform soil moisture data assimilation using observations and improved model simulation results. Hence more emphasis has been given to soil moisture in this paper and the model performance has been evaluated based on that. This model intercomparison study differs from those of the PILPS and GSWP. Unlike the PILPS and GSWP, this study focuses on local-scale hydrologic processes at high spatial and temporal scales over a study location in a humid climate and has the objective to find a better land surface model for soil moisture data assimilation study at local scale.

[6] Description of the models and their physical processes are briefly summarized in section 2. The study area and field observation data sets are described in section 3. Brief description about the model input data sets and the model setup are given in section 4. The model simulation results and discussion are presented in section 5. Finally, the conclusions are provided in section 6.

2. Land Surface Models

[7] There are three LSMs used in this study. They are (1) the Hydrological improvements to the Simplified Version of the Simple Biosphere Model (HySSiB [*Mocko et al.*, 1999; *Sud and Mocko*, 1999]); (2) the National Centers for Environmental Prediction (NCEP) Noah Land Surface Model Version 2.7.1 (Noah 2.7.1, hereafter Noah [*Ek et al.*, 2003]); and (3) the National center for Atmospheric Research (NCAR) Community Land Model Version 3 (CLM3.0, hereafter CLM [*Dai et al.*, 2003]). A summary of the model differences is listed in Table 1. HySSiB and Noah are "second generation" LSMs, primarily concerned with calculation of the surface energy and water balances. CLM is "third generation" in that it also maintains a carbon budget and explicitly represents the controls that photosynthesis exerts on water and energy in the soil-vegetation-atmosphere system. As a basic requirement for any model intercomparison study, all the three models were simulated on the same LIS platform/environment (except CLM) and forced by identical atmospheric forcing and land surface parameters.

2.1. LIS Architecture

[8] The NASA/Goddard Space Flight Center's Land Information System (LIS [*Kumar et al.*, 2006]; http://lis.gsfc.nasa.gov/) is built upon Global (GLDAS [*Rodell et al.*, 2004]) and North American (NLDAS [*Mitchell et al.*, 2004]) Land Data Assimilation Systems (http://ldas.gsfc.nasa.gov). LIS features a high performance and flexible design, provides infrastructure for data integration and assimilation, and operates primarily on an ensemble of land surface models for execution over user-specified regional or global domains. The LIS software is designed within an object-oriented framework, with explicit abstract interfaces defined for customization and extension to different applications. LIS is a flexible and expandable system and it can be customized to incorporate more user defined land surface schemes, atmospheric forcing and land surface parameter data sets. All the land surface models (LSMs) in LIS simulate energy and water variables (e.g., soil moisture (both liquid and frozen), soil temperature, skin temperature, runoff) and fluxes (e.g., evaporation and transpiration) at 1-km (fine) to 25-km (coarse) spatial resolutions, and at one-hour or shorter temporal resolutions [*Zhan et al.*, 2004]. LIS also follows the Assistance for Land Modeling Activities (ALMA [*Polcher*, 2000]) convention, which is a common data and metadata standard used among the land surface community to denote energy and water variables. The version 4.3.2. of LIS is used in this study.

2.2. HySSiB Model

[9] HySSiB is a biophysical model designed to simulate land surface processes realistically and calculate radiation absorption, reflection, and provide fluxes of momentum, and sensible and latent heat [*Mocko and Sud*, 2001]. The original version of the HySSiB (known as SSiB [*Xue et al.*, 1991]) got its lineage from the Simple Biosphere Model (SiB) [*Sellers et al.*, 1986] with reduced physical parameters and improved computational efficiency. A major difference of HySSiB from the original SSiB of *Xue et al.* [1991] is its distinct conceptual architecture of snow pack and radiative transfer through snow. It also includes an orography-based surface runoff scheme and interaction with a water table below the third soil layer. HySSiB includes 3 soil layers with lower boundaries at 2 cm, 150 cm, and 350 cm below the surface. HySSiB considers the rooting depth at 100 cm below the surface [*Oliveira et al.*, 2006]. It has one canopy and one snow layer. It has eight prognostic variables, namely soil wetness in 3 soil layers, water stored on canopy and ground and temperature at the canopy, ground surface and deep soil layers [*Xue et al.*, 1996]. The equation for canopy interception is based on conservation of water. It uses a finite difference approximation and a discretization of Darcy's law for vertical flow of water between soil layers. Soil parameters are a function of a small set of soil types. The drainage of water out of the bottom layer includes the

Table 1. Basic Differences Among the Three Land Surface Models

	HySSiB	Noah	CLM
No. of soil layers	3	4	10
Soil layer boundaries (cm)	2, 150, 350	10, 40, 100, 200	1.8, 4.5, 9.1, 16.6, 28.9, 49.3, 82.9, 138.3, 229.6, 342.3
Model physics	Uses mass conservation law, vertical discretized Darcy's law	Uses mass conservation law, diffusive form of Richard's equation	Water conservation at canopy and soil layer, vertical discretized Darcy's law
Reference	*Mocko and Sud* [2001]	*Ek et al.* [2003]	*Dai et al.* [2003]

water due to gravitational percolation and baseflow suggested by *Liston et al.* [1994]. The temperature of the canopy is based on the energy conservation equation whereas the surface and deep soil temperatures are solved using the force-restore method [*Deardorff*, 1978]. The mass and energy transfers between land surface and atmosphere are represented using a resistance formulation. The water stress term includes the stomatal resistance to the atmosphere, soil water potential and vapor pressure deficit. The stomatal resistance in this model is based on *Jarvis* [1976]. The soil water potential is taken from the empirical relationship of *Clapp and Hornberger* [1978]. The resistance between the canopy and the reference height is based on similarity theory. The resistance to the water transfer from the surface soil layer to the canopy layer includes an aerodynamic resistance and a soil surface resistance. The aerodynamic resistance is based on its relationship to the Richardson number [*Xue et al.*, 1996].

[10] The HySSiB soil layer boundaries and rooting depth are prescribed via a lookup table as a function of vegetation type. The lookup table also includes all of the soil parameters, aerodynamic parameters as well as stomatal resistance coefficients, roughness and canopy heights, vegetation fraction, leaf reflectance and transmittance, greenness, and leaf area index (LAI).

2.3. Noah Model

[11] The Noah LSM gets its lineage from the Oregon State University (OSU) LSM originally developed in the 1980s at OSU [*Mahrt and Pan*, 1984]. It has been upgraded and extended by the National Centers for Environmental Prediction (NCEP) and its collaborators [*Chen et al.*, 1996]. This model has been validated through many model intercomparison studies; both in coupled [*Betts et al.*, 1997; *Ek et al.*, 2003] and uncoupled [*Wood et al.*, 1998; *Schlosser et al.*, 2000; *Robock et al.*, 2003] studies. It has been implemented in operational weather and climate models because of its moderate complexity and computational efficiency. This model has a vertical soil profile that extends two meters below the surface. This vertical profile is partitioned into 4 soil layers with lower boundaries at 10 cm, 40 cm, 100 cm, and 200 cm below the surface. The rooting depth of the Noah model is fixed at 100 cm, which includes top three soil layers. It has one snow layer and one canopy layer. The prognostic variables include soil moisture and temperature in soil layers, water stored on the canopy and the snow stored on the ground [*Chen and Dudhia*, 2001]. The physics of vertical water mass movement between the soil layers is governed by the mass conservation law and the diffusive form of the Richard's law whereas the infiltration is governed by a conceptual parameterization for the sub-grid treatment of precipitation and soil moisture [*Schaake et al.*, 2004]. At the bottom of the soil layers, drainage is only due to gravitational percolation as the hydraulic diffusivity is zero. The total evaporation includes the direct evaporation from the top soil layer, the evaporation from the canopy intercepted water and transpiration. The surface skin temperature is determined from surface energy balance equation representing combined ground-vegetation surface. The soil layer temperature is solved using the Crank-Nicholson scheme. The ground heat flux is determined using diffusion equations for soil temperature [*Chen and Dudhia*, 2001]. This study includes the community version of the one-dimensional Noah model, version 2.7.1.

[12] The Noah model uses a vegetation lookup table for static vegetation parameters such as minimum canopy resistance, solar radiation term for canopy resistance, vapor pressure deficit, threshold snow depth, roughness length and leaf area index. It uses a soil lookup table for static soil parameters. In this case, we used soil types map described in *Zobler* [1986].

2.4. CLM

[13] CLM is a community model that combines features from the Land Surface Model (LSM) of *Bonan* [1996], the Biosphere-Atmosphere Transfer Scheme (BATS) of *Dickinson et al.* [1986] and the 1994 version of the Chinese Academy of Sciences Institute of Atmospheric Physics LSM (IAP94 [*Dai and Zeng*, 1997]). The current CLM includes 10 soil layers with telescoping layer boundaries approximately at 1.8 cm, 4.5 cm, 9.1 cm, 16.6 cm, 28.9 cm, 49.3 cm, 82.9 cm, 138.3 cm, 229.6 cm, and 342.3 cm below the surface. It has one canopy layer and one to five snow layers depending on the snow depth. CLM focuses on biogeophysics of the land surface and includes vegetation dynamics and river routing modules. The water intercepted by canopy is calculated from a mass balance equation. The water flow within the snow layers is by an explicit scheme which permits a portion of liquid water over the holding capacity of snow to percolate into the underlying layer. The water flow from the bottom of the snow layer is available for infiltration into soil and for runoff [*Dai et al.*, 2003]. CLM runoff includes the surface and baseflow. CLM uses the conceptual TOPMODEL (a topography based hydrological model which compromises between fully distributed process complex model and lumped empirical simple models [*Beven et al.*, 1995; *Campling et al.*, 2002]) approach to parameterize the surface run-off and a discretized version of

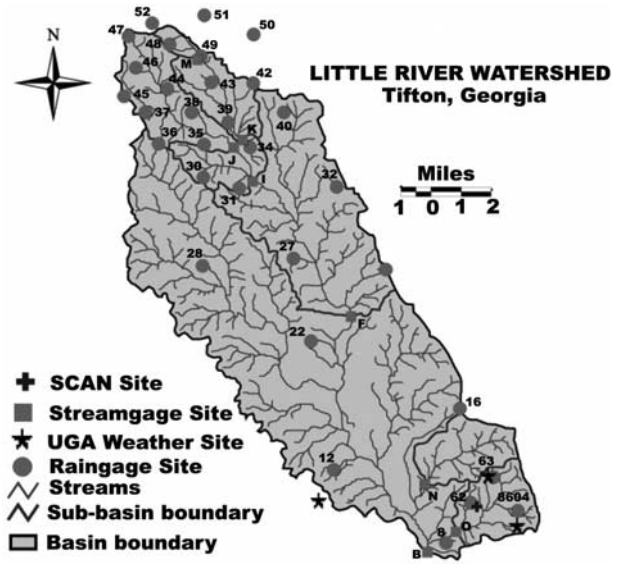

Figure 1. Little River Experimental Watershed (LREW), Tifton, Georgia [from *Cashion et al.*, 2005]. The in-situ soil moisture measuring instruments have been installed at some of the rain-gauge sites.

Darcy's law for vertical downward flow of water within soil layers [*Oleson et al.*, 2004]. The baseflow includes bottom drainage, saturation excess and the subsurface lateral runoff. The ground albedo includes the soil and canopy albedo (and snow over snow surface). It applies a two-stream radiative transfer approximation for canopy albedo [*Sellers and Dorman*, 1987]. Soil albedo is a function of soil color and moisture. The snow albedo is a function of snow age, grain size, solar zenith angle, pollution and the amount of fresh snow. The vapor flux between the reference height and the canopy is calculated iteratively using Monin-Obukhov similarity theory [*Bonan et al.*, 2002]. Total evapotranspiration includes the evaporation from the canopy intercepted water, transpiration through vegetation and direct evaporation from the ground. The canopy temperature is calculated by solving the foliage energy conservation equation using the Newton-Raphson iteration method. The soil and snow heat transfer is based on the heat diffusion equation. The heat flux at the surface is calculated using the energy balance equation at the surface where as the heat flux at sub-surface is described by the Fourier law for heat conductance and the heat flux value is zero at the bottom of the soil column.

[14] CLM addresses sub-grid variability through the use of tiles. Each grid cell is divided into any number of tiles, each tile consisting of a single land cover type. Each vegetation land cover includes up to four plant functional types (PFTs [*Bonan et al.*, 2002]). Energy and water balances are calculated separately for each tile at each time step. The tiles interact directly with the mean atmospheric grid condition over the respective tiles, but do not interact with each other. The values over a grid box are areally weighted averages of all the tiles inside the grid [*Dai et al.*, 2003].

[15] Like HySSiB and Noah, CLM also uses a vegetation lookup table for time invariant vegetation parameters. These include the ratio of momentum roughness length to canopy top height, ratio of displacement height to canopy height, characteristic of leaf dimension, photosynthetic pathway, maximum rate of carboxylation at 25°C, slope of conductance to photosynthesis relationship and quantum efficiency at 25°C, visible and infra-red reflectance and transmittance from leaf and stem, leaf orientation index and rooting distribution parameter. This study includes the version 3.0 of the CLM.

[16] Some of the equivalent features among the three models are that (1) all three models used for this study conserve energy and water at each time step and (2) they also use the discretized Darcy's law for vertical water movement between soil layers. The major differences are (1) number of soil and snow layers (SSiB has 3 soil and 1 snow layer, Noah has 4 soil and 1 snow layer, CLM has 10 soil and 5 snow layers); (2) complexity of the models (CLM is a complex third generation model where as HySSiB and Noah are second generation models); and (3) parameterization (each model uses its own soil and vegetation lookup table for soil and vegetation static values for different soil and vegetation types). In contrast to Noah and CLM, HySSiB does not use the input soil data set (described in section 4.2), but finds all the soil parameters from the lookup table as a function of vegetation type.

3. Description of Study Area and In-Situ Data Sets

3.1. Study Area

[17] The Little River Experimental Watershed (LREW) located near Tifton, Georgia (Figure 1) is one of the four designated watersheds selected to calibrate and validate the AMSR-E satellite soil moisture observations. It has high temporal and spatial resolution in-situ soil moisture observations. The watershed encompasses 334 km^2 area, including seven gauged sub-watersheds ranging in size from 3 to 115 km^2. It is in the headwaters of the Suwannee River Basin that begins in Georgia and empties into the Gulf of Mexico. The Little River is a tributary of the Withlacoochee River which is one of the two main tributaries of the Suwannee River. The LREW has flat topography with broad flood plains [*Sheridan*, 1997].

[18] The watershed land use is a mixture of row-crop agriculture, pasture and forage production, upland and riparian forest. It consists of approximately 36% forest, 40% crops, 18% pasture, and the remaining area is wetlands and residential areas. The major crops in the area are peanuts and cotton. Other crops include tobacco, corn, soybeans, melons and some vegetable crops. Swamp hardwoods with thick vegetation occur along the stream edges [*Bosch et al.*, 2006]. Extensive land use information and physical characteristics of this LREW have been described in *Williams* [1982], *Sheridan and Ferreira* [1992], and *Perry et al.* [1999]. The dominant soil type is sandy loam that has a sandy surface layer and loamy subsoil. Most of the soils are well drained and they have fairly low water holding capacities (10 to 30%) [*Hubbard et al.*, 1985].

[19] The area experiences long, hot, humid summers and short mild winters. The average annual precipitation is approximately 1200 mm. Precipitation in this region is poorly distributed and typically occurs in short duration

high-intensity thunderstorms with relatively small spatial extent during the summer months [*Bosch et al.*, 1999].

[20] There is a network of 35 tipping bucket precipitation gauges located within the LREW which record the cumulative rainfall every 5 minutes. The spacing between the precipitation gauges varies from three to eight km (Figure 1). There is also a Soil Climate Analysis Network (SCAN) site available within the watershed, described in detail below. As a part of the AMSR-E calibration and validation project, a network of Steven-Vitel hydra probe soil moisture instruments (http://www.stevenswater.com/soil_moisture_sensors/index.aspx) have been installed at some rain gauge sites since 2001 to monitor soil water continuously at 5-, 20-, and 30-cm depths [*Cashion et al.*, 2005]. The detailed description of the soil moisture measuring sites can be found in *Bosch et al.* [2006]. Soil water measurements are taken at half hour intervals at these sites to conform to the SCAN data. This watershed was also a part of the Soil Moisture Field Experiment conducted in June and July 2003 (SMEX03).

3.2. LREW In-Situ Observation Data

[21] Field observation data were collected by the United States Department of Agriculture - Agricultural Research Service (USDA-ARS) located at Beltsville, MD [*Jackson et al.*, 2006]. The data include instant soil moisture from top 5 cm, instant soil temperature and cumulative precipitation data at every 30-minute interval for the year of 2003 from 17 individual stations located within the LREW (Figure 1). The data also include some statistics such as mean and standard deviation of instant soil moisture, instant soil temperature and cumulative precipitation over all the 17 stations in each 30-minute interval. Limited quality control and quality assurance have been carried out by USDA-ARS. Arithmetic averages and averages based on nearest neighbor weighting are done on the basis of the same set of sensors and several sensors have been eliminated from this averaging by USDA because of poor or suspicious performance. The detailed description of these in-situ data can be found in the work of *Jackson et al.* [2006].

3.3. SCAN Data

[22] SCAN is a nationwide comprehensive soil moisture system which have been collecting and providing soil moisture and soil temperature as well as precipitation, solar radiation, air temperature, specific humidity, wind speed and direction data for longer periods of time [*Schaefer and Paetzold*, 2001]. The measured data are first automatically validated against the preset limits and then manually checked. Measurements of soil moisture at 5-, 10-, 20-, 50-, and 100-cm soil depths are taken wherever possible. This network is distributed mostly over the agriculture areas of USA. The data can be obtained from the USDA Natural Resources Conservation Service Web site (http://www.wcc.nrcs.usda.gov/scan/). As mentioned earlier, there is only one SCAN site available within the LREW (Station 2027, Little River, Georgia, 31.50°N and 83.55°W). Since this SCAN site provides most of the meteorological forcing data, we used this SCAN site data to validate the North American Land Data Assimilation System (NLDAS) forcing data needed to drive LSMs. These NLDAS forcing data have been used as input for all land surface model simulations carried out in this study.

4. Input Data and Model Setup

4.1. Forcing Data

[23] We did not have adequate observed forcing data from the field experiments to drive the model simulations. So, North American Land Data Assimilation System (NLDAS) forcing data were used for the model simulations here. It is a model-observation combined forcing data product. NLDAS data provide hourly measurements at 1/8-degree spatial scale over the North America from 30 September 1996 to present. The data include air temperature and specific humidity at 2-m height, wind speed at 10-m height, surface pressure, downward shortwave and longwave radiation, convective available potential energy, skin temperature, total and convective precipitation and photosynthetically active radiation. It is based on a backbone of Eta Data Assimilation System (EDAS) and is supplemented with observations for two major forcing fields: precipitation and incoming solar radiation [*Cosgrove et al.*, 2003]. The precipitation observations in the NLDAS data are derived from a combination of daily National Center for Environmental Prediction (NCEP) Climate Prediction Center (CPC) gauge based precipitation analyses [*Higgins et al.*, 2000] and hourly National Weather Service Doppler Radar (WSR-88D) precipitation analyses. The hourly radar data are used to temporally disaggregate the daily CPC precipitation data into hourly scale [*Cosgrove et al.*, 2003]. NLDAS incoming solar radiation observation data are derived from Geostationary Operational Environmental Satellite (GOES) data [*Pinker et al.*, 2003]. *Luo et al.* [2003] performed a comprehensive validation study for the NLDAS data sets using the station observations over the Southern Great Plains (SGP). They found a high bias in the NLDAS downward shortwave radiation, but a low bias in the downward longwave radiation; hence cancellation provides a lower bias in total incoming radiation. They also found most meteorological fields other than wind speed agreed very well with observations. Most importantly, they found the differences between LSM simulations with the input NLDAS forcing versus station observations were not primarily due to the atmospheric forcing, but the differences among physics between the models.

[24] The findings of *Luo et al.* [2003] give us confidence that the NLDAS atmospheric forcing data sets will be adequate for our study here. Since we have a single SCAN site available within our study region and the SCAN instrument provides meteorological data sets along with the soil moisture data, we also performed a validation study for the NLDAS forcing data. Figure 2 shows the scatter plots of the hourly meteorological data sets (downward shortwave radiation, precipitation, air temperature and wind speed) from NLDAS and SCAN for the year 2003. Downward longwave radiation was not available from the SCAN site. The bias, root mean square difference (RMSD) and the correlation have also been given for the comparison of each forcing variable. In general, the forcing variables are in good agreement with the SCAN observed data. The most notable difference between the two data sets is in the downward shortwave radiation. It has a relatively large

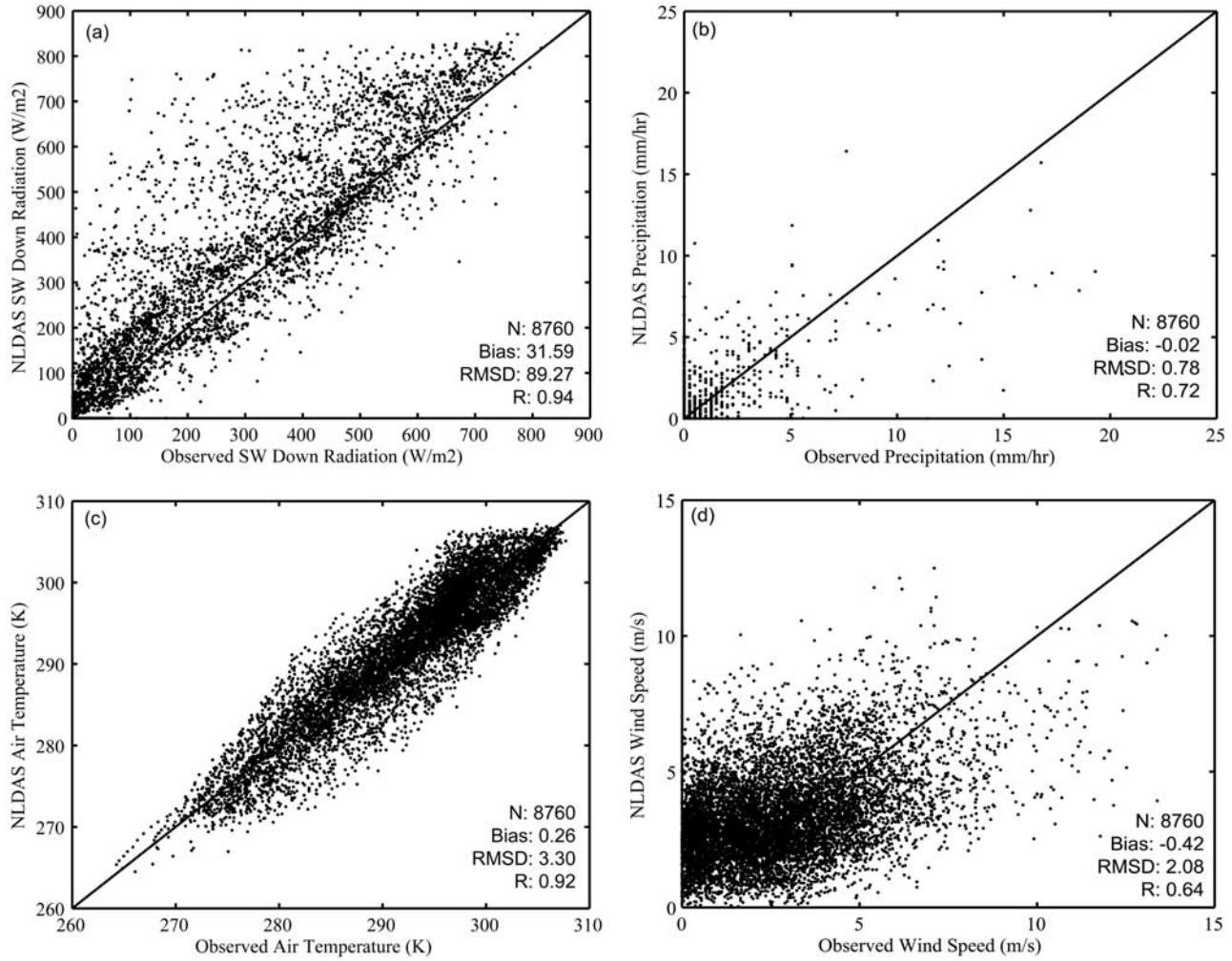

Figure 2. Scatter plots of hourly atmospheric forcing from NLDAS and SCAN measurements at SCAN site for the year 2003. (a) Downward shortwave radiation (W/m^2), (b) total precipitation (mm/hour), (c) air temperature (K), and (d) wind speed (m/s).

RMSD and a notable high bias relative to the SCAN shortwave radiation data (Figure 2a). *Luo et al.* [2003] found similar behavior of the NLDAS incoming shortwave radiation and attributed those differences with the in-situ observations to morning cloud cover conditions. The SCAN hourly precipitation data sets show higher precipitation rates than the NLDAS hourly precipitation rates for heavy precipitation events (Figure 2b). This is because NLDAS derives hourly precipitation from daily totals. We also drew daily time series for precipitation comparisons. The time series plot of daily precipitation from NLDAS and SCAN shows a better match between both the data sets (with RMSD 0.78 mm/hr) except for few large daily precipitation rates (Figure 3). The air temperature (Figure 2c) data sets match very well with the SCAN instrument observations. Wind speed (Figure 2d) data sets for NLDAS and SCAN vary considerably but the differences are not as systematic as is the case with the incoming shortwave radiations. These findings agree well with those of *Luo et al.* [2003].

4.2. Parameter Data

[25] The primary land surface parameters are concerned with vegetation (land cover, greenness) and soil (texture, color, etc.). For land cover, we use the University of Maryland's (UMD) 1-km global land cover product [*Hansen et al.*, 2000]. This data set has a total of 13 land cover classes excluding water bodies. The land-sea mask was also generated from this vegetation classification map. For soil, the sand, silt and clay fraction and soil color data were generated at 1-km resolution from the original Food and Agriculture Organization (FAO) 5-minute resolution global soil maps. These above data sets were used for the simulations of all the models except the soil data set. Soil data were used only by the Noah model and CLM. HySSiB model uses a lookup table to find out the soil information as a function of vegetation type. LIS uses GTOPO30 Digital Elevation Model (DEM) elevation data from US Geological Survey (USGS). LIS does the elevation correction by adjusting the forcing data whenever the elevation differs between LIS and the atmospheric model which produced the atmospheric forcing data. All three models were integrated using the same soil and vegetation parameter data sets, but the procedures used to estimate model parameters were model specific. The Noah model required additional parameters such as a quarterly albedo climatology, monthly greenness fraction climatology, maximum snow albedo, and bottom

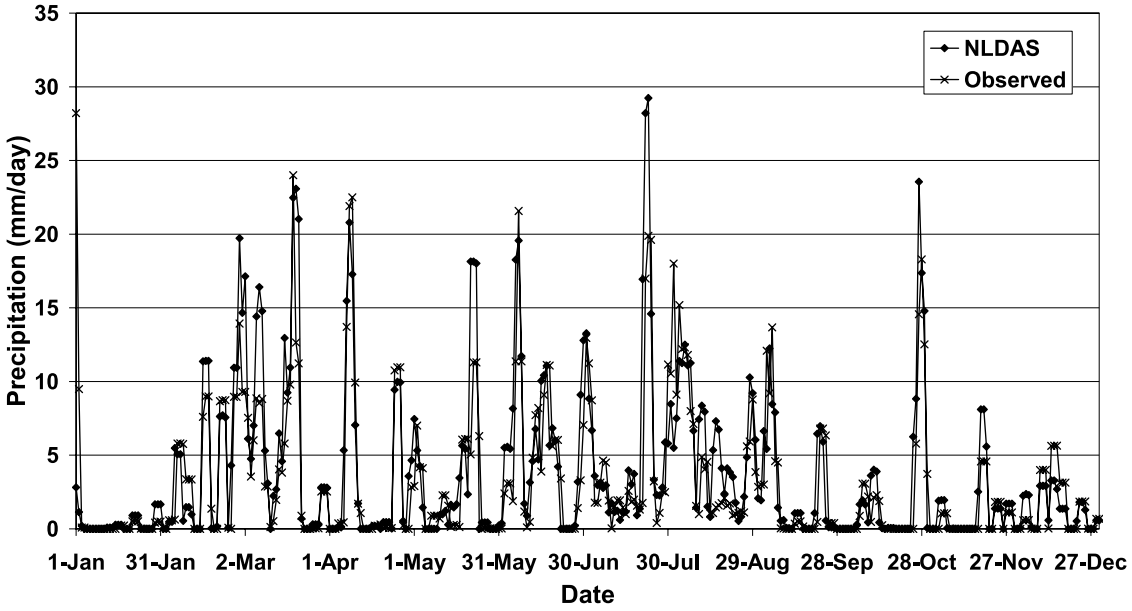

Figure 3. Time series plot of daily precipitation (mm/day) from NLDAS and SCAN measurements at SCAN site for the year 2003.

temperature without elevation correction. Similarly, CLM required canopy height and vegetation classification lookup tables, Leaf Area Index (LAI) and Stem Area Index (SAI) data sets. For the calculation of the LAI climatology, the Moderate Resolution Imaging Spectroradiometer (MODIS) 1-km LAI data were preferred over the Advanced Very High-Resolution Radiometer (AVHRR) 16-km LAI data because of the better spatial resolution in the earlier one. The MODIS LAI data were collected from Boston University [*Yang et al.*, 2006]. The SAI climatology was calculated from LAI data using the methods described in *Sellers et al.* [1996] and *Los et al.* [2000].

4.3. Model Initialization

[26] Improper model initialization can produce erroneous model output results. We adopted one of the model initialization methods described in *Rodell et al.* [2005]. NLDAS input forcing data are available from October 1996. We used five years of NLDAS input forcing data (from January 1997 to December 2002) to spin up the model state variables by looping three times through the 5 years of forcing data (a total 15 years of spin-up). Then the climatology state was calculated from the mean of the outputs of five January months of the last five years to produce initialization conditions for 1 January 2003. This approach is one of the better ways of initializing a land surface model to reduce the occurrence of unrealistic extremes in the initialization [*Rodell et al.*, 2005].

4.4. Model Simulation

[27] All three models were integrated retrospectively from 1 January to 31 December 2003 at 1-km spatial resolution over a region bounded by 83.38°–84°W longitude and 31.11°–31.88°N latitude (62 × 77 km domain). The model time step was 15 minutes with model output saved every hour. The NLDAS retrospective forcing was hourly, so forcing variables were interpolated to 15-min intervals. The solar zenith angle interpolation scheme based on the solar zenith angle was used for this temporal interpolation to avoid the error introduced by a simple linear interpolation scheme. Table 2 shows the details of the model setup.

5. Results and Discussion

5.1. Scale Issues and Preprocessing of Results

[28] The simulation results from the three models have been compared for all simulated variables except the surface soil moisture where we also used the in-situ observations. It is important to discuss the issues associated with spatial, temporal and vertical resolutions when we are comparing soil moisture data sets from different sources. The field measurements were carried out at point scale whereas the models simulated the land surface processes averaged over 1-km spatial grids. So, instead of comparing the point observations with the grid averaged model simulations, we created a composite average of all the observed data from all the stations in the watershed and compared this composite soil moisture with the averaged soil moisture from all the corresponding grid points for each LSM. A similar kind of approach has also been used when data were from multiple sources [e.g., *Vinnikov and Yeserkepova*, 1991; *Entin et al.*, 2000; *Robock et al.*, 2003; *Schaake et al.*, 2004; *Reichle et al.*, 2004; *Prigent et al.*, 2005]. Also, this region is topographically very flat and the soil moisture spatial variation is not large over this region [*Cashion et al.*, 2005]. Thus spatial averaging of soil moisture over this watershed is reasonable for this study. We had complete soil moisture observations from 8 measurement stations for the year 2003. So, we also used corresponding 8 model grids for this comparison study. For all other model-simulated variables, we also used the spatial averaging for same 8 grids to reduce any model uncertainties at local grid scale.

[29] The model simulation outputs were at 1-hour interval and the in-situ soil moisture observations were at 30-minute interval. However, for energy cycle variables, we used daily

Table 2. Initial Model Setup for the GLDAS/LIS Model Runs

Land surface model (LSM)	Noah, CLM, HySSiB
Base forcing	NLDAS
Land cover type	University of Maryland's global 1-km land cover map
Soil classification map	Food and Agriculture Organization
Maximum number of tiles per grid	13
Time step of the run	15 min
Latitude range	31.11°N to 31.88°N
Longitude range	84.00°W to 83.38°W
Output data resolution	1 km
Output interval to write the output files	1 hr
Output data format	Binary

averaged values and for precipitation we used daily accumulated values instead of instant values for the comparison study. This avoids the strong variability and noise associated at the hourly time scale.

[30] The in-situ soil moisture data are from top 5-cm layer. The top soil layer depth for HySSiB model is 2 cm (surface layer). Similarly the Noah model has 10 cm and CLM model has ~2-cm surface layer depths. We did not change the model soil layer depths for various reasons. First, we wanted to use the default model structure, parameterization and physics for each model for this study. Second, we had discussions with many model developers/users. According to them, if the model top soil layer depth is changed, then it affects other model layers/parameterization and it completely becomes a new model. Hence it requires extensive evaluation and testing before it can be used with changed soil layer thickness. Third, we simulated the Noah model with different top soil layer thickness and compared the results (figure not shown here). We did not find any significant difference in the Noah model results for different top layer thickness when the results were expressed in % vol/vol.

[31] Previous studies have shown very high vertical correlations of soil moisture variability within top 20-cm soil layer [*Wigneron et al.*, 1995; *Calvet et al.*, 1999; *Prigent et al.*, 2005]. We also assumed that the soil moisture variability has very high vertical correlation within top 20-cm soil layer for this study. Without this assumption, it is hard to directly compare the soil moisture data from different models with different top soil layer thickness. At the same time, we recognize the fact that this is a qualitative and crude assumption. So, this assumption can add some source of error in the model intercomparison results.

5.2. Results and Analysis

5.2.1. Soil Moisture

[32] Figure 4 shows the daily time series plots of the top layer soil moisture simulation results from the LSMs (10 cm for Noah, 1.8 cm for CLM and 2 cm for HySSiB) along with the observed Little River Watershed in-situ (5 cm) soil moisture data for the year 2003. Figure 4 also includes the multimodel mean soil moisture, which was calculated taking the arithmetic mean of the three models. It is very clear from this plot that the daily soil moisture peaks from all sources match very well corresponding to daily precipitation peaks (shown in Figure 3). A few interesting points can be noted from Figure 4. First, the models and observations show higher soil moisture during the spring season of the year because of the consistent rainfall events during the spring over this watershed. Second, HySSiB and Noah simulate higher soil moisture values throughout the year compared to observations irrespective of different top soil layer thicknesses for the two models. Third, the CLM soil moisture values are very sensitive to the precipitation forcing as compared to those of other two models and it dries down to a minimum top layer soil moisture threshold value very fast after a precipitation event is over (~couple

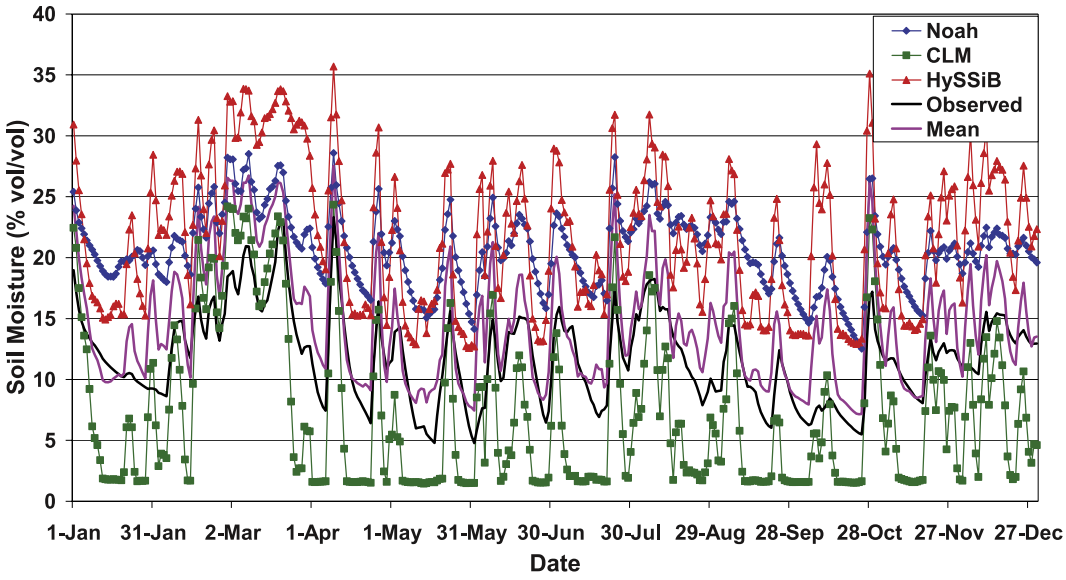

Figure 4. Daily soil moisture time series plots from Noah (10-cm layer), CLM (2-cm layer), HySSiB (2-cm top layer), in-situ measurements (5-cm layer), and Arithmetic Model Ensemble Mean from Noah, CLM, and HySSiB over the Little River Watershed.

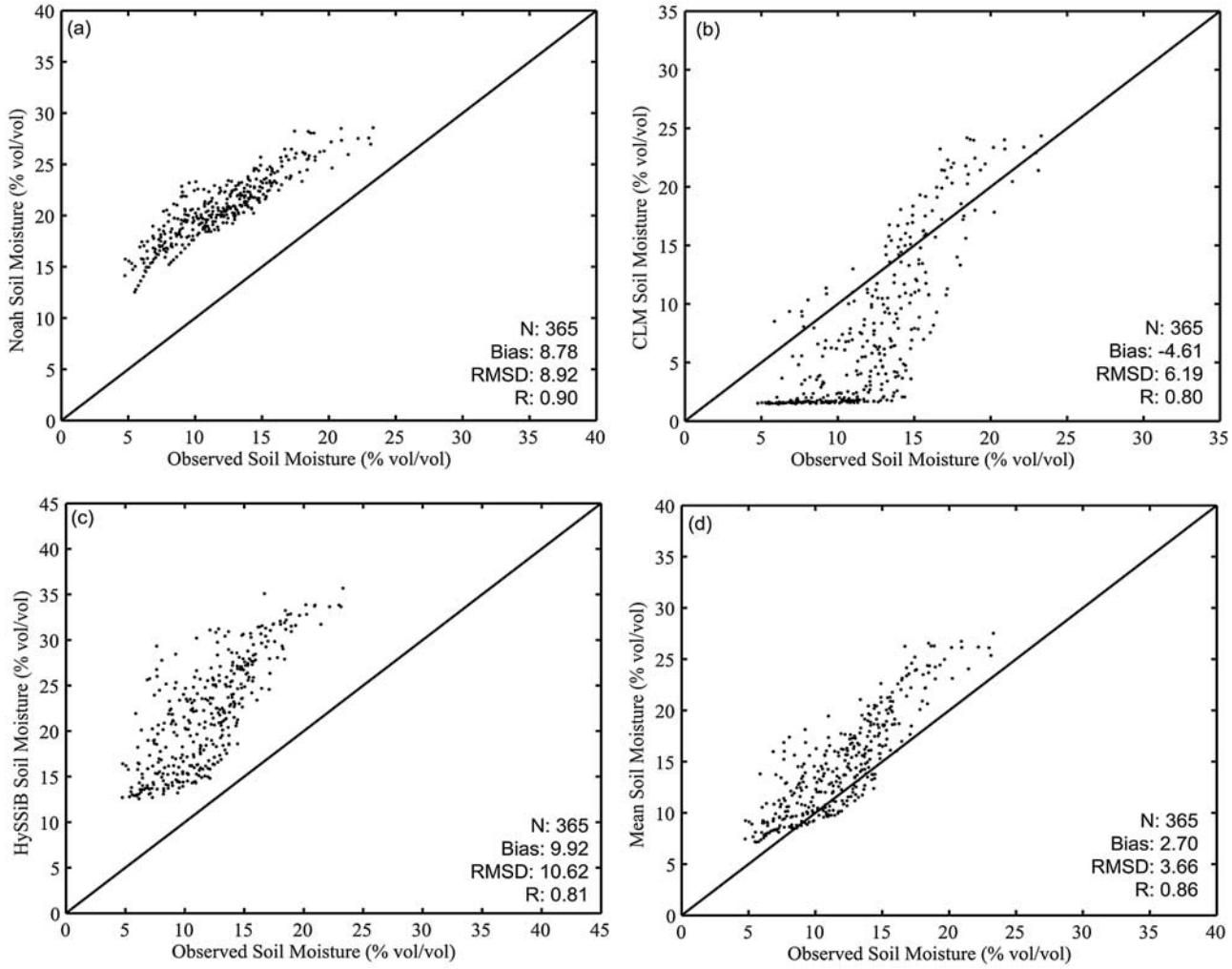

Figure 5. Daily soil moisture scatter plot averaged over eight in-situ stations in the Little River Watershed. (a) Noah versus in-situ, (b) CLM versus in-situ, (c) HySSiB versus in-situ, and (d) Arithmetic Model Ensemble Mean versus in-situ.

of days). This high sensitivity of CLM soil moisture data is because the model soil layer structure has a thin top soil layer. However, HySSiB soil moisture estimates do not show the same behavior as those of the CLM model at daily temporal time scale even though it has an equally thin top layer. Fourth, the model ensemble mean soil moisture performs reasonably well with less bias than any individual model.

[33] To understand the behavior of all the soil moisture estimates, we use scatter plots of the model daily soil moisture simulations along with the model ensemble mean against in-situ observations (Figure 5). A 1:1 line is also shown in each figure for reference. All the comparison statistics for the estimates are calculated with respect to in-situ observations. Figure 5a indicates a high systematic bias (8.78% vol/vol) for Noah. HySSiB also shows high mean bias (9.92% vol/vol) compared to the observations (Figure 5c), but it is not as systematic as that of the Noah model. Because of these high biases, Noah and HySSiB show very high RMSD values; 8.92 and 10.62% vol/vol for Noah and HySSiB model respectively. Yet Noah and HySSiB show high correlations (0.90 and 0.81 for the Noah and HySSiB model respectively) with in-situ observations. In contrast to the other two models, CLM (Figure 5b) has a lower mean bias (-4.61 vol/vol) and RMSD (6.19% vol/vol). The lower threshold value for CLM top layer soil moisture ($\sim$2% vol/vol) is frequently reached (Figure 5b), which is noticeable during the dry down phases in the soil moisture time series plot (Figure 4).

[34] The multimodel ensemble mean shows the lowest mean bias (2.70% vol/vol) and RMSD (3.66% vol/vol). The negative bias in CLM model estimates almost cancels the positive biases in the Noah and HySSiB model estimates, keeping the multimodel ensemble mean bias very low. The correlation values for all data sets range from 0.80 (CLM) to 0.90 (Noah model). The multimodel ensemble mean has comparable correlation value (0.86) as those of the individual model estimates. Since some of the models have systematic high bias even though they have high correlations, we removed the mean biases from all the model simulations and recalculated the RMSD for all the data sets. The RMSD got reduced considerably for the Noah (from

8.92 to 1.60) and HySSiB (from 10.62 to 3.77) soil moisture results in this case (figures not shown in this paper). Moreover, the Noah model estimates scattered around the 1:1 reference line indicating perfect model estimates.

[35] We also looked at the performances of the individual model and multimodel mean soil moisture estimates at individual measuring stations. Figure 6 shows a comparison of the skill scores of the original model-simulated soil moisture products along with the multimodel mean for 8 individual watershed stations and the station-averaged data set. These skill scores are calculated on the basis of hourly soil moisture values for the year 2003 in contrast to the above graphs where we used daily averaged soil moisture values. We will discuss more about the hourly soil moisture estimates later in a separate section. As can be seen, the multimodel mean gives bias (3 to 8% vol/vol), RMSD (5 to 10% vol/vol) and correlation (0.6 to 0.8) skills as good or better than those of the individual model results at each individual observation station as well as for the station average. CLM shows a lower magnitude of bias than the multimodel mean at half the stations and lower RMSD at three stations. Noah shows superiority of time series correlation at all stations. Since any single model is not consistent at all individual sites for all the skill scores, the multimodel mean across all the models provides the best overall estimates in our case. Earlier, *Guo et al.* [2007] considered 17 different model derived soil moisture data products (simple to very complex models) and verified the performance of each model along with the multimodel ensemble mean over Illinois, China, India, Mongolia and Russia. They concluded that the multimodel ensemble mean outperformed most individual products in simulating the phasing of the annual cycle, interannual variability and magnitudes in observed soil moisture. They also found that the multimodel ensemble mean got improved with the inclusion of a product of higher correlation to observations or lower error while there was no degradation in the multimodel ensemble mean when a product with relatively poor skill was included. Our results here supplement the results found by *Guo et al.* [2007]. However, the multimodel mean in our case is calculated only from three land surface models. So, it is not statistically significant to provide any solid conclusion in our case. Hence our findings should not be used as a scientific principle exclusively based on our results.

[36] To analyze the spatial distribution of soil moisture and precipitation-soil moisture coherence patterns, we chose a time period of wetting and drying dynamics (16 to 19 July) over the Little River Experimental Watershed area (approximately 50 km by 75 km area). Figure 7 shows daily NLDAS precipitation forcing (column 1) and corresponding daily soil moisture difference images from Noah (column 2), CLM (column 3) and HySSiB (column 4). All these spatial images are in 1-km spatial resolution. Same color scale has been used for easier visual recognition of the changes in the spatial images. The white region in the precipitation image for 19 July represents the zero precipitation area. Looking at the precipitation panels, there is heavy precipitation in the southeast part on 17 July; in the north-east and central parts on 18 July and complete dry down phase everywhere on 19 July over the watershed. The spatial pattern of soil moisture for all the three models corresponds very well to the spatial distribution of the precipitation events with few exceptions. HySSiB does not show very distinct soil moisture patterns as we see from Noah and CLM though the changes in soil moisture because of precipitation events is still visible in HySSiB simulations. However, the soil moisture difference values are higher (both positive and negative (more than 7% vol/vol)) in HySSiB as compared to the other two models. This indicates that the HySSiB model top layer holds lot of water after precipitation events before it is removed rapidly through infiltration to deeper soil layers and/or evaporative processes.

5.2.2. Water Cycle Variables

[37] Figure 8 shows daily time series plots of other water cycle parameters (surface runoff [Figure 8a], subsurface runoff [Figure 8b] and evaporation [Figure 8c]) from the three models for the year 2003 spatially averaged over the 8 in-situ stations in the Little River Watershed. Each daily surface runoff (Qs) peak (Figure 8a) for all three models corresponds well to each of the precipitation events (Figure 3) indicating direct response of model surface runoff to the precipitation events. Subsurface runoff peaks can be seen corresponding to only heavy precipitation days, especially during frequent precipitation in the spring season. This indicates that all the models have high water holding capacity to retain some water in their soil layers and they produce sub-surface runoff only during high precipitation events. HySSiB immediately produces substantial runoff during heavy precipitation events, losing water through surface runoff before it enters the soil (Figure 8a). At the same time, we have noticed the high top layer soil moisture estimates for HySSiB during precipitation events (Figure 4). Hence HySSiB produces very low subsurface runoff (Figure 8b). Contrast to that, the Noah model has almost no surface runoff (Figure 8a) but it has very high top layer soil moisture (Figure 4). Since the Noah top layer is thick (10 cm), it accommodates greater infiltration and produces more subsurface runoff than HySSiB. In contrast, CLM shows very different characteristics for hydrologic variables estimations. The dry down of CLM soil moisture is compensated by intermediate surface runoff and very high subsurface runoff. This high subsurface runoff during precipitation events could be because CLM subsurface runoff has more pathways than the other models.

[38] The evaporation patterns are also very different among the three models (Figure 8c). All models exhibit the expected seasonal pattern of evaporation, with higher evaporation during the summer and lower evaporation during the winter season. On short time scales, CLM evaporation is very sensitive to the precipitation patterns. Along with the surface and subsurface runoff, evaporation also removes some CLM top layer soil water immediately during the precipitation events. HySSiB shows a similar kind of evaporation pattern as those for CLM. Noah shows comparatively low variability in evaporation estimates than other two models. Hence the evaporation is less from the top layers of CLM and HySSiB and they show many dry-down events during the lower precipitation season (August–October). Moreover, the transpiration through vegetation is also shut down because of low root zone soil moisture for the CLM and HySSiB models. The Noah model holds more water in the top layer due to the thicker

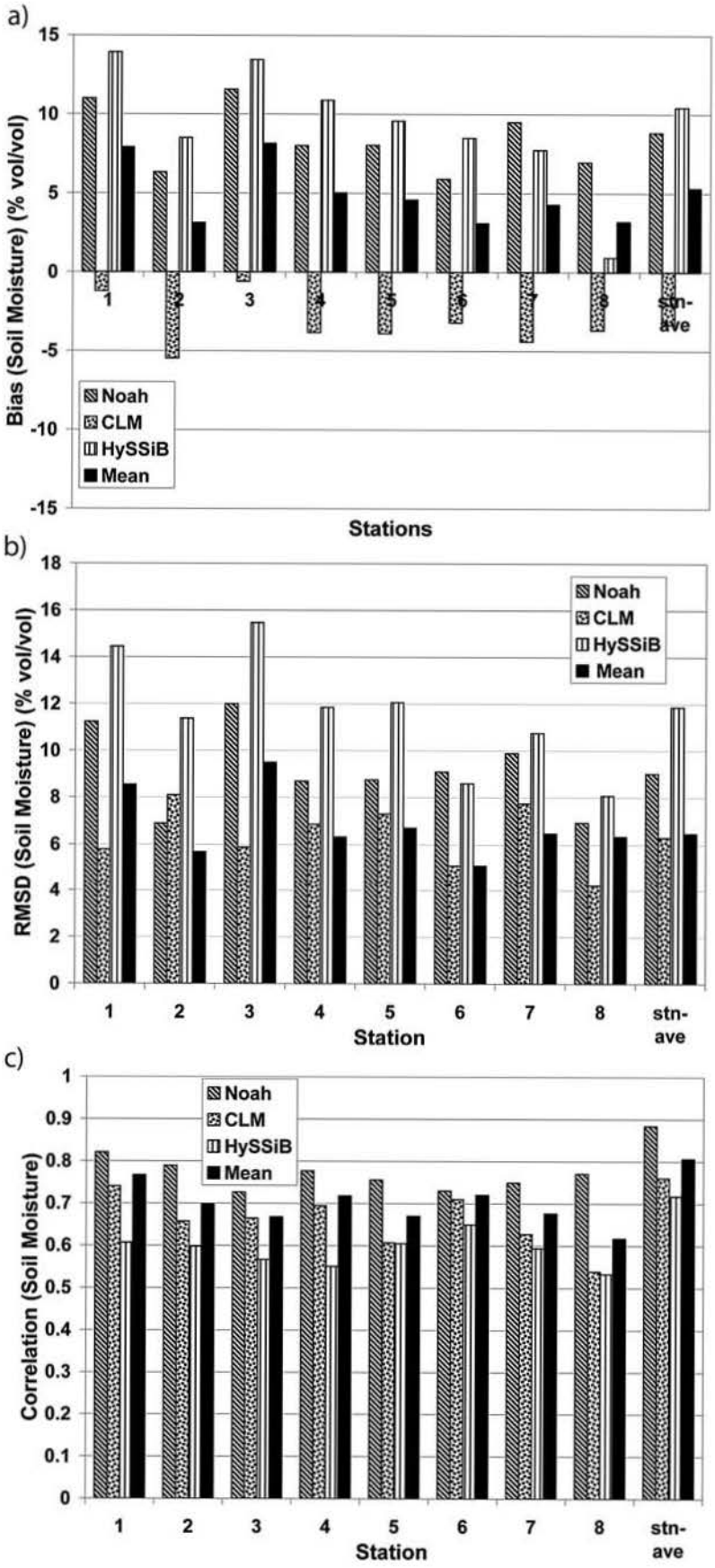

Figure 6. (a) Mean bias, (b) RMSD, and (c) correlation of Noah, CLM, HySSiB, and Arithmetic Model Ensemble Mean soil moisture for eight in-situ stations and station-averaged data set.

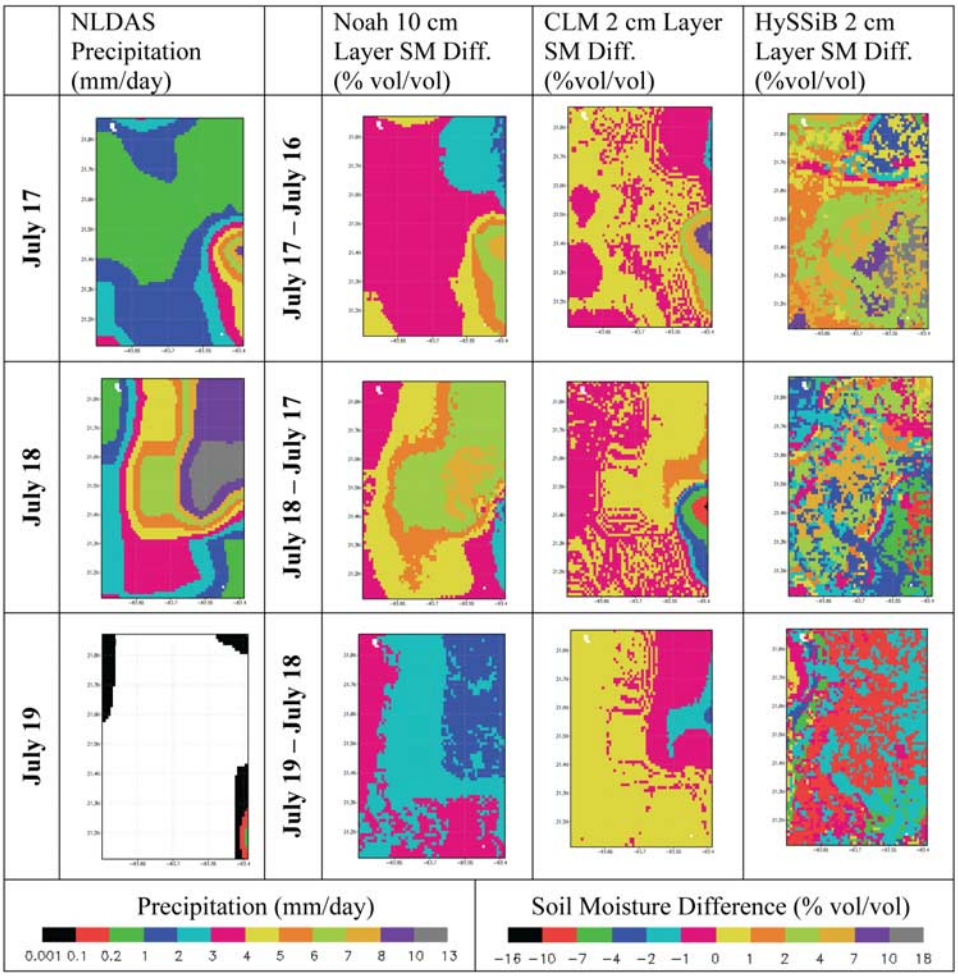

Figure 7. Spatial difference image of NLDAS precipitation and corresponding model-simulated soil moisture results during 16–19 July. There are spatial coherences between the precipitation events and model soil moisture results.

top layer and the evaporation still goes on for the Noah model when the other two models show dry down phases, hence the Noah model shows an opposite behavior to that of the other two models (e.g., 8 to 14 September, 15 to 21 September, 26 September to 6 October in Figure 8c).

5.2.3. Energy Cycle Variables

[39] Figure 9 shows the daily time series plots of the energy budget parameters for the same in-situ stations and time period as in Figure 8. The incoming energy at the earth's surface is indicated with positive sign and the outgoing energy is negative. All models show very similar net solar radiation patterns for the whole time period (Figure 9a). Since downward shortwave radiation is the same for all models, the net solar radiation indirectly represents the albedo values used by the models. The net solar radiation values from all the three models are distinctly different during the spring season (April–June). CLM produces the lowest net surface solar radiation during spring season. This implies that CLM exhibits higher surface albedo than the other two models. During the other seasons, the values are similar to one another. In the case of the net surface longwave radiation, Noah and HySSiB match very closely (Figure 9b). CLM estimates match the other two models except during the phases of top layer soil moisture dry down. During these days, CLM shows increasing soil and surface temperature, which contributes significantly to the lower net longwave radiation.

[40] Figures 9c and 9d represent the daily latent and sensible heat flux. These fluxes reciprocate each other for all three models. Variability of latent and sensible heat flux depends on the amount of energy and water available at the earth's surface. Latent and sensible heat flux variability is very high for CLM as compared to the other two models for this time period. For reasons stated previously, CLM produces relatively high latent heat flux and low sensible heat flux for any precipitation event. On the other hand, Noah has the lowest variability. HySSiB exhibits relatively high variability in heat fluxes. Figure 9e shows the ground heat flux variability from all the three models. Ground heat flux is a residual in the energy budget and contributes to changes in subsurface soil temperature. Noah exhibits the least variability in the ground heat flux, while CLM shows high variability. Since all these land surface models close the energy budget at each time step, the variability of the

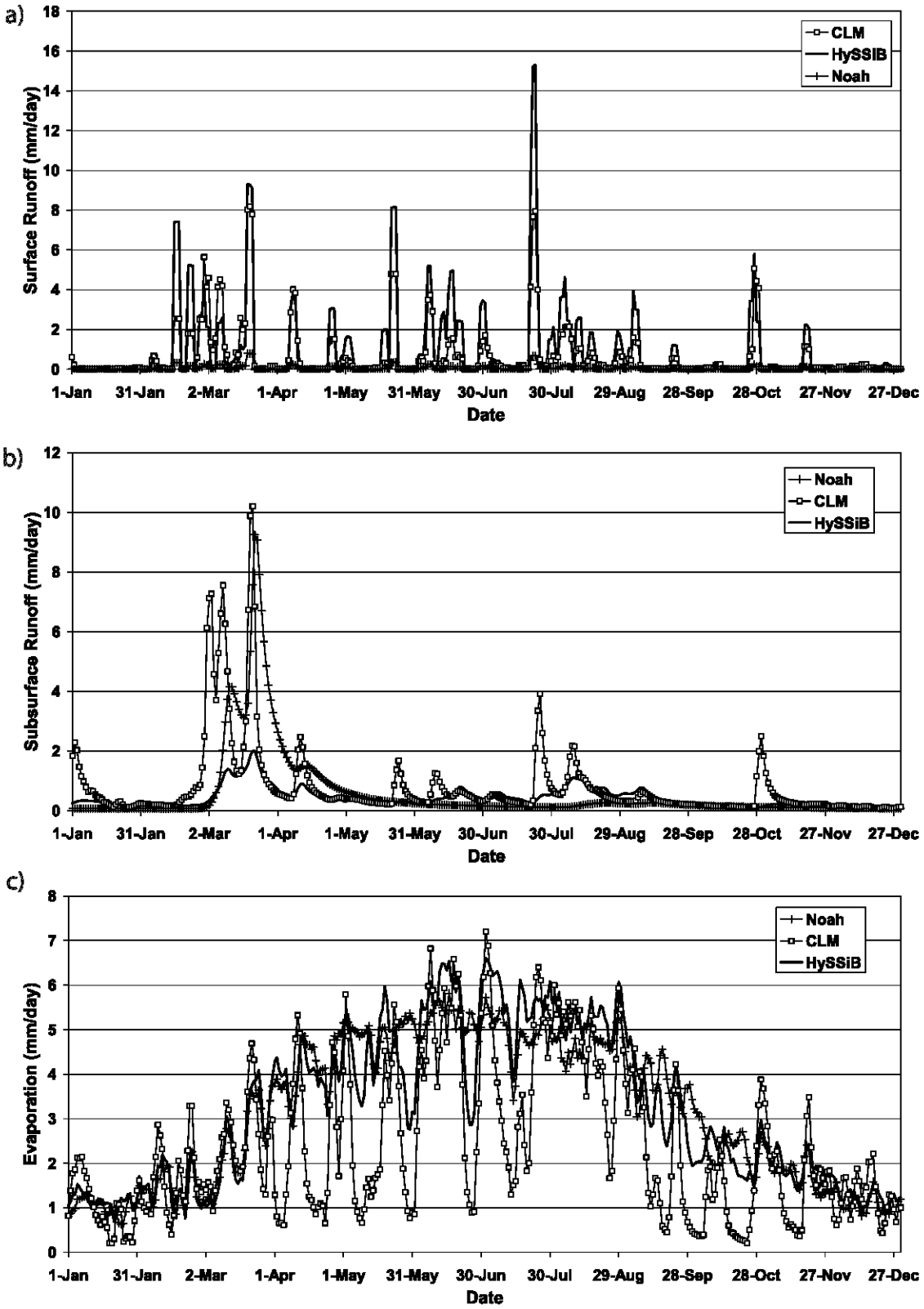

Figure 8. Comparison of water cycle variables simulated by Noah, CLM, and HySSiB (a) Surface runoff (mm/day), (b) subsurface runoff (mm/day), and (c) evaporation (mm/day).

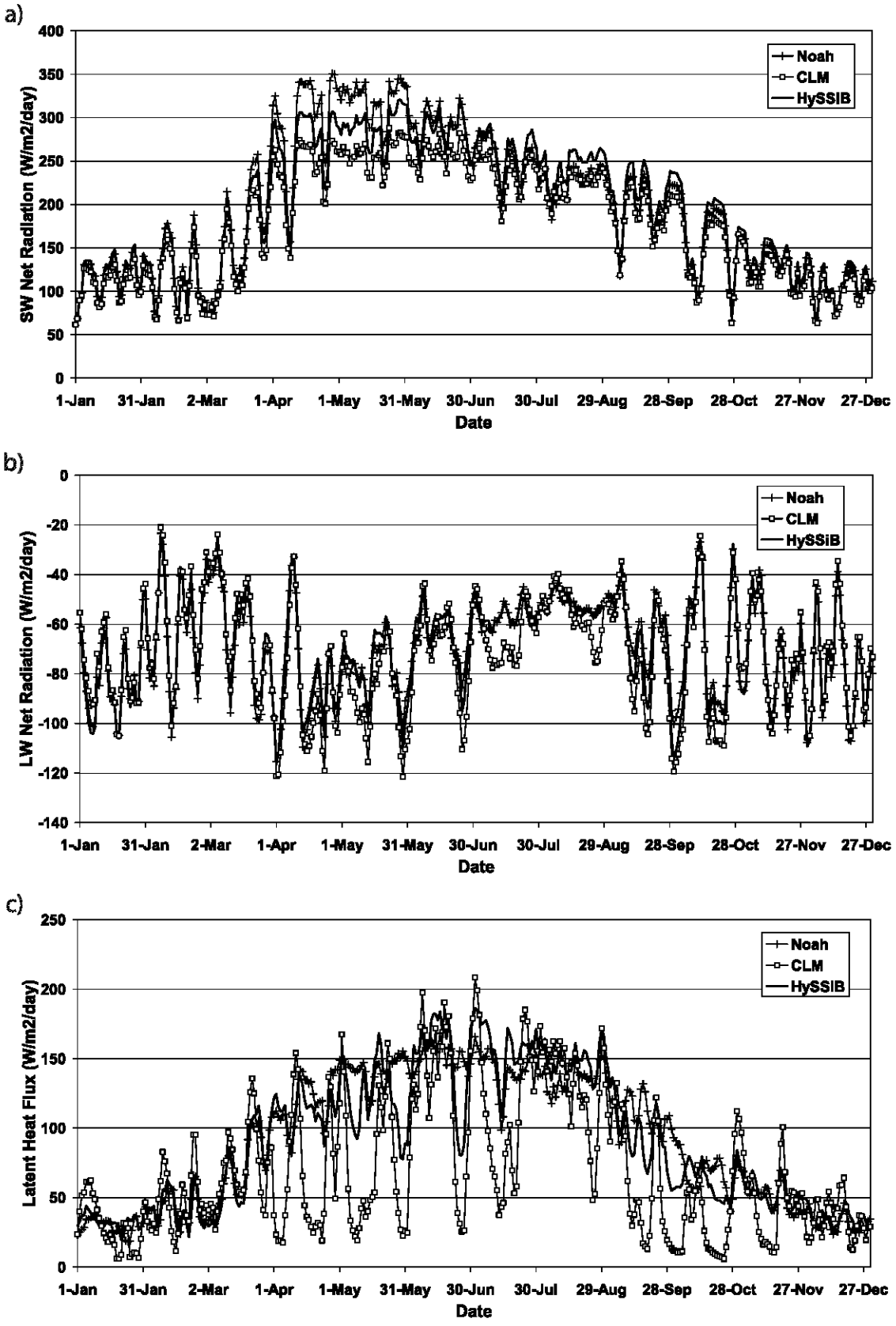

Figure 9. Comparison of energy cycle variables simulated by Noah, CLM, and HySSiB. (a) Net shortwave radiation (W/m^2/day), (b) net longwave radiation (W/m^2/day), (c) latent heat flux (W/m^2/day), (d) sensible heat flux (W/m^2/day), and (e) ground heat flux (W/m^2/day).

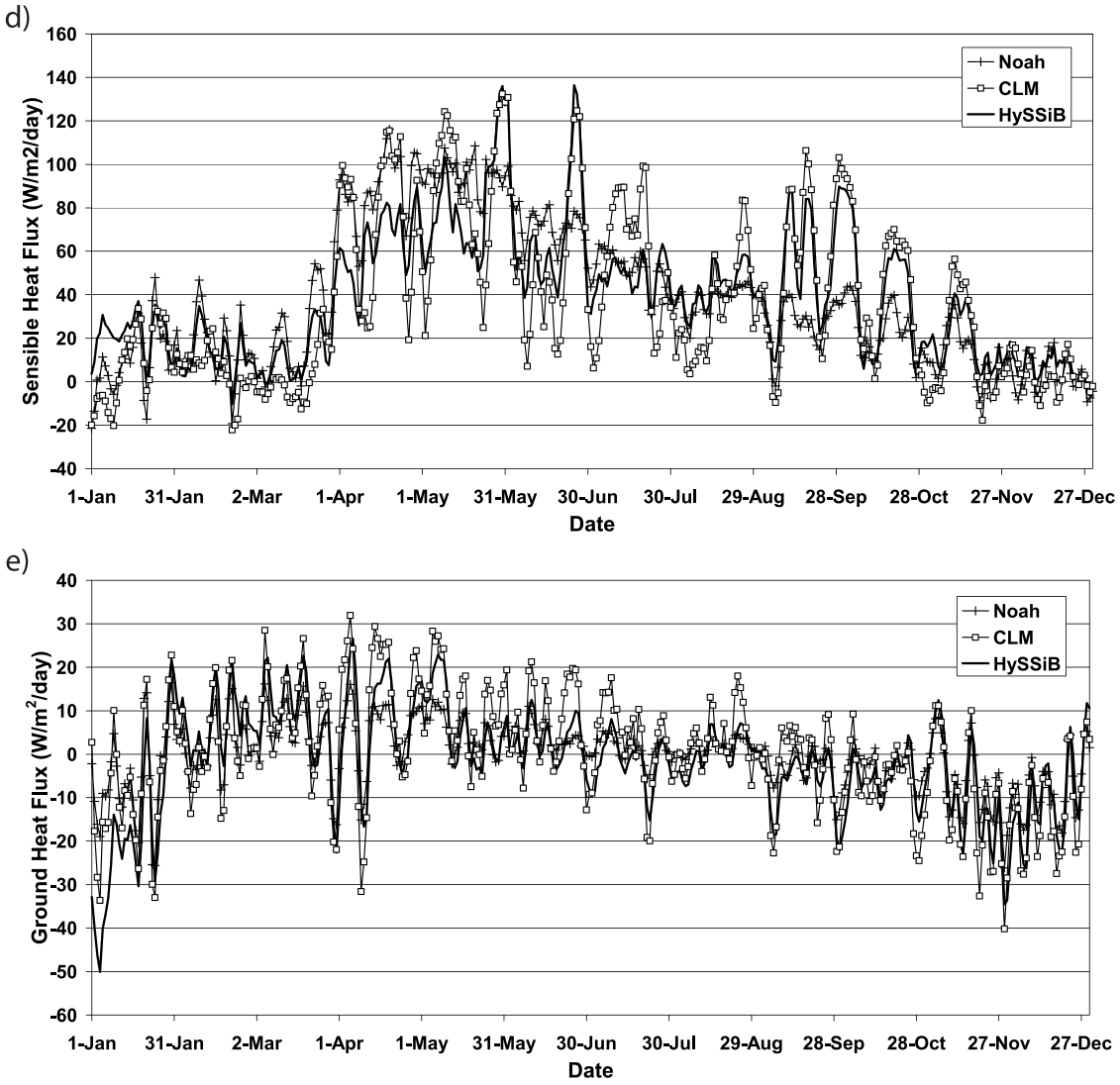

Figure 9. (continued)

ground heat flux depends on the variability of other energy budget parameters. In winter months, the ground loses heat to the atmosphere in all three models. This indicates that the total incoming energy flux is less than the total outgoing energy flux in winter season; spring and summer show the opposite situation.

5.3. Impact of Scaling on Soil Moisture

[41] *Boone et al.* [2004] discussed the impact of spatial scaling on model-simulated water and energy cycle parameters. In this section, we discuss temporal scaling of the model soil moisture simulations. As shown in section 5.2.1, there exist systematic biases in some LSMs on daily time scales. Our objective in this section is to look at the original hourly soil moisture model outputs in contrast to the daily soil moisture simulations and provide our critical comments from data assimilation point of view. Figure 10 shows the scatter plot of the hourly soil moisture data from 3 individual models and their arithmetic ensemble mean against the in-situ observations for the year 2003. The corresponding daily soil moisture scatter plots were shown in Figure 5. Compared to the daily soil moisture data, the Noah model hourly soil moisture data show very similar behavior with systematic high bias and high correlation (Figure 10a). The lower threshold bound can very clearly be seen for CLM hourly soil moisture data in Figure 10b. CLM model hourly soil moisture data also exhibit similar characteristics as those of the daily soil moisture data with much scatter that does not appear to reflect a simple systematic bias. In the case of the HySSiB model, the hourly simulated soil moisture data show a very clear lower threshold boundary around 7% vol/vol which is not apparent in the daily soil moisture scatter plots because of the scaling of hourly values to daily values (Figure 10c). This characteristic of HySSiB at hourly scale resembles that of the CLM model. This confirms that the sensitivity of the top layer soil moisture to the precipitation events is due to the soil layer parameterization since we see this complete dry down phase in CLM and HySSiB model (both have 2-cm top soil layer), but not in case of the Noah (10-cm soil layer) model. HySSiB seems to exhibit the diurnal cycle of surface soil moisture incorrectly, but does well at the daily time scale. CLM has problems with both diurnal and synoptic dry-

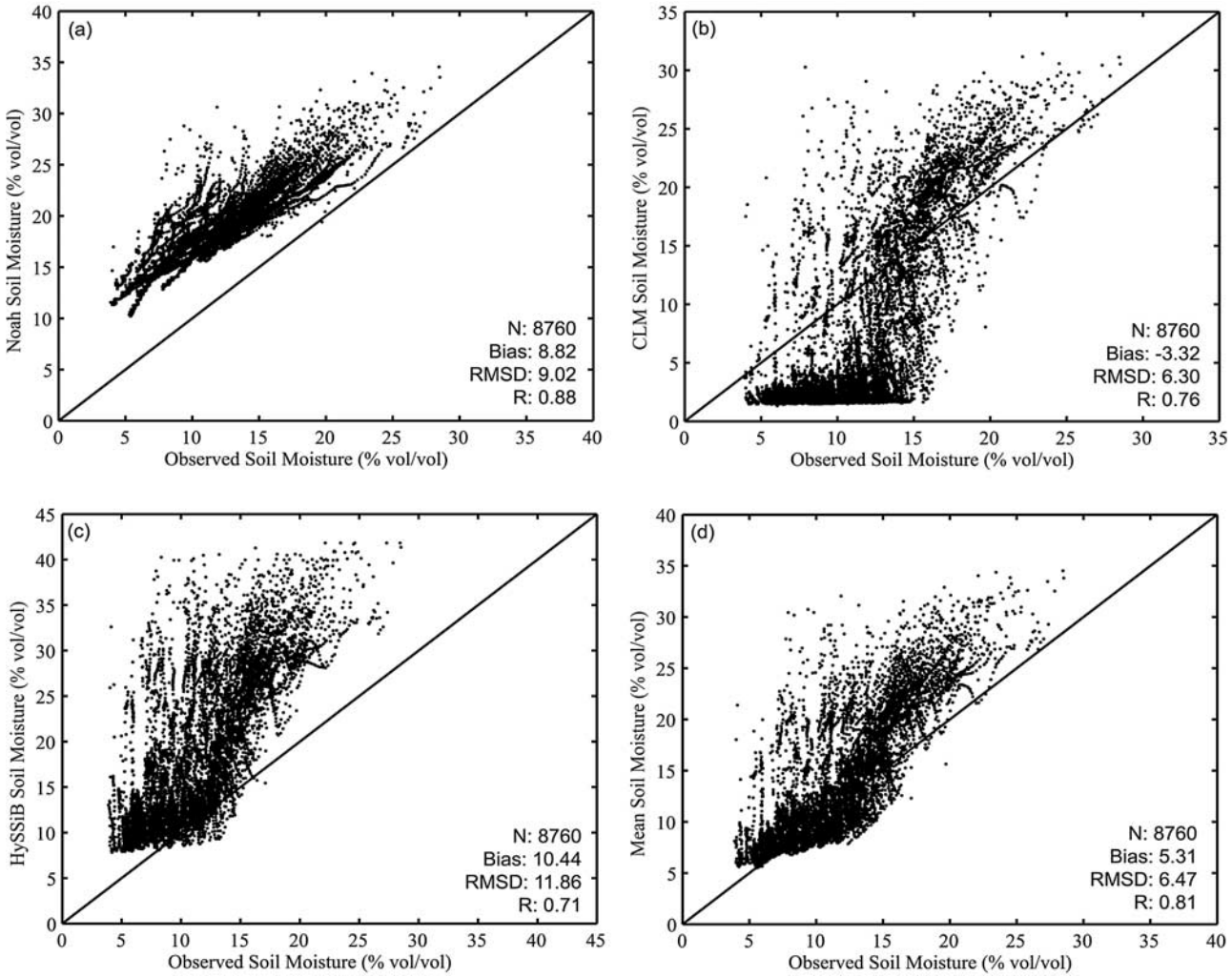

Figure 10. Same as Figure 5 but for hourly soil moisture data.

down phases. The hourly multimodel mean (Figure 10d) shows similar behavior as for the mean daily data (Figure 5d). For all the soil moisture products, the mean bias and RMSD are higher (except CLM mean bias) and the correlation is lower at hourly scale than those at daily scale. This is expected since the uncertainty for soil moisture at hourly scale is supposed to be higher than that at the daily scale. Table 3 shows the statistics from these comparisons, along with the results after a simple bias correction for each model. Bias correction reduces RMSD by 70% or more when dry-down phases are well modeled.

6. Conclusion

[42] In this paper, we performed comparison studies of water and energy cycle variables simulated by three different land surface models. The offline simulations were conducted using HySSiB, Noah and CLM land surface models driven by NLDAS atmospheric forcing data over the Little River Watershed, Georgia region from October 1996 to September 2003. The model simulation results for the year 2003 were compared to the in-situ observations. Important differences among the three land surface models were the complexity of the models, the top soil layer thickness and the layer parameterizations in each model. When NLDAS precipitation forcing was compared with the corresponding SCAN measured meteorological parameters, we found reasonable agreement among the data sets from the two sources. Model simulations at 1-km spatial resolution and hourly temporal resolution were good enough to look at the model responses to individual precipitation events and compare simulation results from the three models.

[43] All the three land surface models simulated soil moisture realistically and exhibited close correspondence in soil moisture results to each precipitation event in space and time. The model layer parameterization played a major role in soil moisture simulation results at hourly scale. CLM was found to be overly sensitive to climatic conditions. CLM and HySSiB both overestimated the magnitude of surface soil moisture variations on dry-down time scales. The scatter plots of the individual model and the arithmetic model ensemble mean soil moisture against the in-situ observed soil moisture were conducted irrespective of the location of the in-situ sites. The model mean performed well at the hourly and daily scale. The multimodel mean soil moisture also provided comparable skill scores with those of any individual model even at individual in-situ measuring

Table 3. Skill of Hourly and Daily Time Series Simulations of Soil Moisture

	Hourly				Daily			
	Bias	RMSD	Bias Corrected RMSD	RMSD Reduction (%)	Bias	RMSD	Bias Corrected RMSD	RMSD Reduction (%)
Noah	8.82	9.02	1.88	79	8.78	8.92	1.60	82
CLM	−3.32	6.30	5.36	15	−4.61	6.19	4.13	33
HySSiB	10.44	11.86	5.63	53	9.92	10.62	3.17	70
Multimodel mean	5.31	6.47	3.69	43	2.70	3.66	2.47	33

sites, while avoiding some of the systematic problems exhibited by individual models. Our results supplement the results found by *Guo et al.* [2007] though it should not be used as a scientific principle exclusively based on our findings since our multimodel ensemble mean is derived only from three models.

[44] The models showed discrepancies in partitioning the precipitation water into soil moisture, surface runoff, infiltration and evaporation terms. CLM compensated low top layer soil moisture by high surface and subsurface runoff. On the other hand, Noah maintained high top layer soil moisture by near zero surface and lower subsurface runoff. HySSiB produced high top layer soil moisture and surface runoff, but very low subsurface runoff. All models exhibited very similar results in net solar radiation and longwave radiations. CLM simulated higher albedo as well as higher surface temperatures. Model physics played a critical role in partitioning the outgoing energy into latent heat and sensible heat fluxes pertaining to different climatic conditions. Models did not agree well in partitioning of latent and sensible heat fluxes.

[45] We had some difficulties in performing this kind of comparison study. First, there were no in-situ observations available for most of the water and energy cycle variables to compare with the model simulation results. Second, the NLDAS downward shortwave radiation showed high biases whereas the NLDAS precipitation forcing values were lower for most of the heavy precipitation events as compared to those of the SCAN instrument observations. Since we had the precipitation observations for all the collocated in-situ soil moisture measurement sites, we chose just one site (RG63) and replaced the precipitation field in the NLDAS forcing data with the in-situ observed precipitation data and re-ran all the three models for that specific point location only. We found that the model soil moisture values were higher in the new simulations (figures not shown here) because the in-situ precipitation data had higher values than those of the NLDAS precipitation values. However, the nature of the soil moisture data for all the three models remained same because both the NLDAS precipitation and the in-situ observed precipitation data detected all the precipitation events at the same time/day of the year but with different values (figure not shown here). Hence we believe that the agreement or disagreement among the model-simulated results found in this paper is mostly due to the different treatments of land surface processes by different schemes. From the point of view of soil moisture data assimilation, high time-resolution simulations with good quality soil moisture estimates and comparable observation measurements are required. From the hourly scatter plots, it can be seen that Noah soil moisture with the mean bias removed can serve as the best model for a data assimilation study. Noah appears to be the least likely model to "fight against" the assimilation of observations. However, when we look at the Noah model parameterization, it has a 10-cm-thick top soil layer where as most of the available remote sensing soil moisture products are from only the top 2 cm of soil. This inconsistency may be an important factor to consider while performing the data assimilation. In the case of CLM and HySSiB, the model soil discretizations agree better with the character of remote sensing observations, but these model results are not as well behaved compared to the Noah model. It is hard to say at this point which plays a more important role in data assimilation: better model simulation behavior or the choice of model soil layer discretization. This question can be answered in future studies by performing some data assimilation tests with these model simulations.

[46] Modeling studies of local-scale land surface processes help us to understand the land surface with the goal of realizing its local-scale applications in water resource management, climate prediction and disaster mitigation. The results produced here also motivate us to look further into land surface model complexity and physics, external factors like atmospheric forcing and land surface parameters, and to estimate the relative contribution of each factor on these local-scale processes in our future study.

[47] **Acknowledgments.** The valuable contributions made by the three anonymous reviewers to improve this manuscript are highly appreciated. We are thankful to the LIS software team, particularly Jim Geiger for his technical support to use the LIS system and the LSMs. We would also like to acknowledge Hiroko Kato for providing her support to use the Grid Analysis and Display System (GrADS) and to run the LSMs. We are grateful to Mike Cosh in USDA-ARS Laboratory at Beltsville, Maryland, for providing all the in-situ measurement data sets used in this study. We thank Roshan Shrestha of CREW for providing the model code to replace the NLDAS precipitation with the in-situ observations in LIS. Paul Dirmeyer's participation was made possible under the Independent Research/Development provisions of NSF grant ATM-0610629.

References

Betts, A. K., F. Chen, K. E. Mitchell, and Z. I. Janjic (1997), Assessment of the land surface and boundary layer models in two operational versions of the NCEP Eta Model using FIFE data, *Mon. Weather Rev.*, *125*, 2896–2916.

Beven, K. J., R. Lamb, P. F. Quinn, R. Romanowicz, and J. Freer (1995), TOPMODEL, in *Computer Models of Watershed Hydrology*, edited by V. P. Singh, pp. 627–668, Water Resources Publications, Highlands Ranch, Colo.

Bonan, G. B. (1996), A land surface model (LSM version 1.0) for ecological, hydrological, and atmospheric studies: Technical description and user's guide, *NCAR Tech. Note NCAR/TN-417+STR*, Natl. Cent. for Atmos. Res., Boulder, Colo.

Bonan, G. B., K. W. Oleson, M. Vertenstein, S. Levis, X. Zeng, Y. Dai, R. E. Dickinson, and Z.-L. Yang (2002), The land surface climatology of the Community Land Model coupled to the NCAR Community Climate Model, *J. Clim.*, *15*, 3123–3149.

Boone, A., et al. (2004), The Rhone-Aggregation Land Surface Scheme Intercomparison Project: An overview, *J. Clim.*, *17*, 187–208.

Bosch, D. D., J. M. Sheridan, and F. M. Davis (1999), Rainfall characteristics and spatial correlation for the Georgia Coastal Plain, *Trans. ASAE*, *42*(6), 1637–1644.

Bosch, D. D., V. Lakshmi, T. J. Jackson, M. Choi, and J. M. Jacobs (2006), Large scale measurements of soil moisture for validation of remotely sensed data: Georgia soil moisture experiment of 2003, *J. Hydrol.*, *323*, 120–137.

Calvet, J. C., et al. (1999), MUREX: A land-surface field experiment to study the annual cycle of the energy and water budgets, *Ann. Geophys.*, *17*, 838–854.

Campling, P., A. Gobin, K. Beven, and J. Feyen (2002), Rainfall-runoff modeling of a humid tropical catchment: The TOPMODEL approach, *Hydrol. Process.*, *16*, 231–253.

Cashion, J., V. Lakshmi, D. Bosch, and T. J. Jackson (2005), Microwave remote sensing of soil moisture: Evaluation of the TRMM microwave imager (TMI) satellite for the Little River Watershed Tifton, Georgia, *J. Hydrol.*, *307*(1–4), 242–253.

Chen, F., and J. Dudhia (2001), Coupling an advanced land surface-hydrology model with the Penn State-NCAR MM5 modeling system. part II: Preliminary model validation, *Mon. Weather Rev.*, *129*, 587–604.

Chen, F., K. Mitchell, J. Schaake, Y. Xue, H.-L. Pan, V. Koren, Q. Duan, M. Ek, and A. Betts (1996), Modeling of land surface evaporation by four schemes and comparison with FIFE observations, *J. Geophys. Res.*, *101*, 7251–7266.

Clapp, R. B., and G. M. Hornberger (1978), Empirical equations for some soil hydraulic properties, *Water Resour. Res.*, *14*, 601–604.

Cosgrove, B. A., et al. (2003), Real-time and retrospective forcing in the North American Land Data Assimilation System (NLDAS) project, *J. Geophys. Res.*, *108*(D22), 8842, doi:10.1029/2002JD003118.

Dai, Y., and Q. Zeng (1997), A land surface model (IAP94) for climate studies. part I: formulation and validation in off-line experiments, *Adv. Atmos. Sci.*, *14*, 433–460.

Dai, Y., et al. (2003), The Common Land Model, *Bull. Am. Meteorol. Soc.*, *84*, 1013–1023.

Deardorff, J. W. (1978), Efficient prediction of a ground surface temperature and moisture with inclusion of a layer of vegetation, *J. Geophys. Res.*, *83*, 1889–1903.

Dickinson, R. E., A. Henderson-Sellers, P. J. Kennedy, and M. F. Wilson (1986), Biosphere-Atmosphere Transfer Scheme (BATS) for the NCAR community climate model, *NCAR Tech. Note, TN-275+STR*, 69 pp., National Center for Atmospheric Research, Boulder, Colo.

Dirmeyer, P. A. (1995), Problems in initializing soil wetness, *Bull. Am. Meteorol. Soc.*, *76*, 2234–2240.

Dirmeyer, P. A. (2004), Soil moisture—Muddy prospects for a clear definition, *GEWEX News*, *14*(3), 11–12.

Dirmeyer, P. A., A. J. Dolman, and N. Sato (1999), The Global Soil Wetness Project: A pilot project for global land surface modeling and validation, *Bull. Am. Meteorol. Soc.*, *80*, 851–878.

Dirmeyer, P. A., X. Gao, M. Zhao, Z. Guo, T. Oki, and N. Hanasaki (2006), The Second Global Soil Wetness Project (GSWP-2): Multi-model analysis and implications for our perception of the land surface, *Bull. Am. Meteorol. Soc.*, *87*, 1381–1397.

Ek, M., K. Mitchell, L. Yin, P. Rogers, P. Grunmann, V. Koren, G. Gayno, and J. Tarpley (2003), Implementation of Noah land-surface model advances in the NCEP operational mesoscale Eta model, *J. Geophys. Res.*, *108*(D22), 8851, doi:10.1029/2002JD003296.

Entin, J. K., A. Robock, K. Y. Vinnikov, S. E. Hollinger, S. Liu, and A. Namkhai (2000), Temporal and spatial scales of observed soil moisture variations in the extratropics, *J. Geophys. Res.*, *105*, 11,865–11,877.

Guo, Z., P. A. Dirmeyer, X. Gao, and M. Zhao (2007), Improving the quality of simulated soil moisture with a multi-model ensemble approach, *Q. J. R. Meteorol. Soc.*, *133*, 731–747.

Hansen, M. C., R. S. Defries, J. R. G. Sohlberg, and R. Sohlberg (2000), Global land cover classification at 1 km spatial resolution using a classification tree approach, *Int. J. Remote Sens.*, *21*, 1331–1364.

Henderson-Sellers, A., A. J. Pitman, P. K. Love, P. Irannejad, and T. H. Chen (1995), The project for inter-comparison of land surface parameterization schemes (PILPS): Phases 2 and 3, *Bull. Am. Meteorol. Soc.*, *76*(4), 489–503.

Higgins, R. W., W. Shi, and E. Yarosh (2000), Improved United States precipitation quality control system and analysis, in *Atlas 7*, 40 pp., Natl. Cent. for Environ. Predict./Clim. Predict. Cent., Camp Springs, Md.

Hubbard, R. K., C. R. Berdanier, H. F. Perkins, and R. A. Leonard (1985), *Characteristics of Selected Upland Soils of the Georgia Coastal Plain*, 72 pp., ARS-37, USDA Agricultural Research Service, Tifton, Ga.

Jackson, T. J., M. H. Cosh, X. Zhan, D. D. Bosch, M. S. Seyfried, P. J. Starks, T. O. Keefer, and V. Lakshmi (2006), Validation of AMSR-E soil moisture products using watershed networks, paper presented at International Geoscience and Remote Sensing Symposium, pp. 432–435, Denver, Colo., 31 July–4 August.

Jarvis, P. G. (1976), The interpretation of the variations in leaf water potential and stomatal conductance found in canopies in the field, *Philos. Trans. R. Soc. Lond., B*, *273*, 593–610.

Kumar, S. V., et al. (2006), LIS—An interoperable framework for high resolution land surface modeling, *Environ. Model. Softw.*, *21*, 1402–1415.

Liston, G. E., Y. C. Sud, and E. F. Wood (1994), Evaluating GCM land surface hydrology parameterizations by computing river discharge using a runoff routing model: Application to the Mississippi basin, *J. Appl. Meteorol.*, *33*, 394–405.

Los, S. O., et al. (2000), A global 9-yr biophysical land surface data set from NOAA AVHRR data, *J. Hydrometeorol.*, *1*, 183–199.

Luo, L., et al. (2003), Validation of the North American Land Data Assimilation System (NLDAS) retrospective forcing over the southern Great Plains, *J. Geophys. Res.*, *108*(D22), 8843, doi:10.1029/2002JD003246.

Mahrt, L., and H.-L. Pan (1984), A two-layer model of soil hydrology, *Bound.-Lay. Meteorol.*, *29*, 1–20.

Mitchell, K. E., et al. (2004), The multi-institution North American Land Data Assimilation System (NLDAS): Utilizing multiple GCIP products and partners in a continental distributed hydrological modeling system, *J. Geophys. Res.*, *109*, D07S90, doi:10.1029/2003JD003823.

Mocko, D. M., and Y. C. Sud (2001), Refinements to SSiB with an emphasis on snow physics: Evaluation and validation using GSWP and Valdai data, *Earth Interact.*, *5*, 1–31.

Mocko, D. M., G. K. Walker, and Y. C. Sud (1999), New snow-physics to complement SSiB. part II: Effects on soil moisture initialization and simulated surface fluxes, precipitation, and hydrology of GEOS II GCM, *J. Meteorol. Soc. Jpn.*, *77*(1B), 349–366.

Oleson, K. W., et al. (2004), Technical description of the Community Land Model (CLM), *NCAR Tech. Note, TN-461+STR*, 174 pp., Boulder, Colo.

Oliveira, R., M. Oyama, and C. Nobre (2006), Incorporating hydraulic redistribution (HR) into the Simplified Simple Biosphere model (SSiB), paper presented at 8 ICXHMO, pp. 935–938, Foz do Iguacu, Brazil, 24–28 April.

Perry, C. D., G. Vellidis, R. Lowrance, and D. L. Thomas (1999), Watershed-scale water quality impacts of riparian forest management, *J. Water Resour. Plan. Manage.*, *125*, 117–126.

Pinker, R. T., et al. (2003), Surface radiation budgets in support of the GEWEX Continental Scale International Project (GCIP) and the GEWEX Americas Prediction Project (GAPP), including the North American Land Data Assimilation System (NLDAS) Project, *J. Geophys. Res.*, *108*(D22), 8844, doi:10.1029/2002JD003301.

Polcher, J. (2000), GLASS implementation underway, *GEWEX News*, *10*, 9.

Prigent, C., F. Aires, W. B. Rossow, and A. Robock (2005), Sensitivity of satellite microwave and infrared observations to soil moisture at a global scale: Relationship of satellite observations to in situ soil moisture measurements, *J. Geophys. Res.*, *110*, D07110, doi:10.1029/2004JD005087.

Reichle, R. H., R. D. Koster, J. Dong, and A. A. Berg (2004), Global soil moisture from satellite observations, land surface models, and ground data: Implication for data assimilation, *J. Hydrometeorol.*, *5*, 430–442.

Robock, A., et al. (2003), Evaluation of the North American Land Data Assimilation System over the southern Great Plains during the warm season, *J. Geophys. Res.*, *108*(D22), 8846, doi:10.1029/2002JD003245.

Rodell, M., et al. (2004), The global land data assimilation system, *Bull. Am. Meteorol. Soc.*, *85*(3), 381–394.

Rodell, M., P. R. Houser, A. A. Berg, and J. S. Famiglietti (2005), Evaluation of 10 methods for initializing a land surface model, *J. Hydrometeorol.*, *6*, 146–155.

Sahoo, A. K., P. R. Houser, C. Ferguson, E. F. Wood, P. A. Dirmeyer, and M. Kafatos (2008), Evaluation of AMSR-E soil moisture results using the in-situ data over the Little River Experimental Watershed, Georgia, *Remote Sens. Environ.*, *112*(6), 3142–3152.

Schaake, J. C., et al. (2004), An intercomparison of soil moisture fields in the North American Land Data Assimilation System (NLDAS), *J. Geophys. Res.*, *109*, D01S90, doi:10.1029/2002JD003309.

Schaefer, G. L. and R. F. Paetzold (2001), SNOTEL (SNOwpack TELemetry) and SCAN (Soil Climate Analysis Network), in *Proc. Intl. Workshop on Automated Wea. Stations for Appl. in Agr. and Water Resour Mgmt.*, World Meteorological Organization, AGM-3 WMO/TD 1074. (ftp://ftp.wcc.nrcs.usda.gov/downloads/factpub/soils/SNOTEL-SCAN.pdf)

Schlosser, C. A., A. G. Slater, A. Robock, A. J. Pitman, K. Y. Vinnikov, A. Henderson-Sellers, N. A. Speranskaya, K. Mitchell, and the PIPLS 2(d) contributors (2000), Simulations of a boreal grassland hydrology at Valdai, Russia: PILPS Phase 2 (d), *Mon. Weather Rev.*, *128*, 301–321.

Sellers, P. J., and J. L. Dorman (1987), Testing the Simple Biosphere model (SiB) using point micrometeorological and biophysical data, *J. Clim. Appl. Meteorol.*, *26*, 622–651.

Sellers, P. J., C. J. Tucker, G. J. Collatz, S. O. Los, C. O. Justice, D. A. Dazlich, and D. A. Randall (1996), A revised land surface parameterization (SiB2) for atmospheric GCMS. part II: The generation of global fields of terrestrial biophysical parameters from satellite data, *J. Clim.*, *9*, 706–737.

Sellers, P. J., Y. Mintz, Y. C. Sud, and A. Delcher (1986), A Simple Biosphere model (SiB) for use within general circulation models, *J. Atmos. Sci.*, *43*, 505–531.

Sheridan, J. M. (1997), Rainfall-streamflow relations for coastal plain watersheds, *Appl. Eng. Agric.*, *13*(3), 333–344.

Sheridan, J., and V. A. Ferreira (1992), Physical characteristic and geomorphic data for Little River Watersheds, Georgia, in *USDA-ARS, Southeast Watershed Research Lab., Rep. 099201*, 19 pp., US Department of Agriculture-Agricultural Research Service (USDA-ARS), Tifton, GA.

Sud, Y. C., and D. M. Mocko (1999), New snow-physics to complement SSiB. part I: Design and evaluation with ISLSCP Initiative I data sets, *J. Meteorol. Soc. Jpn.*, *77*, 335–348.

Vinnikov, K. Y., and I. B. Yeserkepova (1991), Soil moisture: Empirical data and model results, *J. Clim.*, *4*, 66–79.

Wigneron, J.-P., A. Chanzy, J.-C. Calvet, and N. Bruguier (1995), A simple algorithm to retrieve soil moisture and vegetation biomass using passive microwave measurements over crop fields, *Remote Sens. Environ.*, *51*, 331–341.

Williams, R. G. (1982), Little River watersheds land use characteristics, in *USDA-ARS, SEWRL Lab., Note 098201*, 20 pp., US Department of Agriculture-Agricultural Research Service (USDA-ARS), Tifton, Ga.

Wood, E., et al. (1998), The Project for Intercomparison of Land-surface Parameterization Schemes (PILPS) Phase 2 (c) Red-Arkansas River basin experiment. I: Experimental description and summary intercomparisons, *Global Planet. Change*, *19*, 115–136.

Xue, Y., F. J. Zeng, and C. A. Schlosser (1996), Sensitivity to soil properties—A case study using HAPEX-Mobility data, *Global Planet. Change*, *13*, 183–194.

Xue, Y., P. J. Sellers, J. L. Kinter III, and J. Shukla (1991), A simplified biosphere model for global climate studies, *J. Clim.*, *4*, 345–364.

Yang, W., et al. (2006), MODIS leaf area index products: From validation to algorithm improvement, *IEEE Trans. Geosci. Remote Sens.*, *44*(7), 1885–1898.

Zhan, X., P. R. Houser, J. P. Walker, and M. Rodell (2004), Validation of AMSR-E soil moisture product using data assimilation techniques, paper presented at COAA 2004, Beijing, 28–30 June.

Zobler, L. (1986), A world soil file for global climate modeling, *NASA Tech. Memorandum 87802*, 32 pp.

P. A. Dirmeyer, Center for Ocean-Land-Atmosphere Studies, IGES, 4041 Powder Mill Rd, Suite 302, Calverton, MD 20705, USA.

P. R. Houser, Center for Research on Environment and Water, IGES, 4041 Powder Mill Rd, Suite 302, Calverton, MD 20705, USA.

M. Kafatos and A. K. Sahoo, College of Sciences, George Mason University, Mail Stop: 6C3, 4400 University Drive, Fairfax, VA 22030, USA. (aksahoo2004@gmail.com)